The Pharma Innovation Journal 2023; SP-12(11): 1641-1646

www.ThePharmaJournal.com

The Pharma Innovation

ISSN (E): 2277-7695
ISSN (P): 2349-8242
NAAS Rating: 5.23
TPI 2023; SP-12(11): 1641-1646

www.thepharmajournal.com
Received: 22-09-2023
Accepted: 29-10-2023

Navrose Sangha
Ph.D. Scholar, Department of Veterinary Pathology, Guru Angad Dev Veterinary and Animal Sciences University, Ludhiana, Punjab, India

Charan Kamal Singh
Retired Senior Veterinary Pathologist, Department of Veterinary Pathology, Guru Angad Dev Veterinary and Animal Sciences University, Ludhiana, Punjab, India

Kuldip Gupta
Head-Cum-Professor, Department of Veterinary Pathology, Guru Angad Dev Veterinary and Animal Sciences University, Ludhiana, Punjab, India

Corresponding Author:
Navrose Sangha
Ph.D. Scholar, Department of Veterinary Pathology, Guru Angad Dev Veterinary and Animal Sciences University, Ludhiana, Punjab, India

Histopathological diagnosis of mesenchymal tumors with foldscope and conventional microscope

Navrose Sangha, Charan Kamal Singh and Kuldip Gupta

Abstract
The current study compares images of mesenchymal tumors produced by foldscope and traditional microscope. A total of 100 biopsy samples were analyzed, out of which 29 cases of mesenchymal tumors were found, included five cases of hemangiosarcoma and lipoma, four cases each of leiomyosarcoma, osteosarcoma, fibroma, fibrosarcoma and three cases of chondrosarcoma. Notably, the foldscope utilized in this study had a magnification equivalent to 200X of conventional microscope. The results of this study underscore the effectiveness of foldscope as a dependable diagnostic instrument for the swift and precise examination of mesenchymal tumors. This advancement holds the potential to accelerate the diagnosis of such tumors, providing substantial advantages to both clinical practice and patient care.

Keywords: Conventional microscope, mesenchymal tumors, foldscope, histopathological examination

Introduction
The Foldscope, an optical microscope engineered by Manu Prakash at Stanford University (Cybulski *et al.*, 2014) [5], constitutes an innovative and economically viable instrument for the expeditious visualization of diverse tissue specimens. Fabricated from polypropylene paper, a spherical glass lens and a diffuser panel, the foldscope provides a lightweight and cost-effective solution amenable to fieldwork applications. The apparatus facilitates the accommodation of microscope slides, permitting their scrutiny by facilely maneuvering them along the foldscope's paper folds. Moreover, the foldscope exhibits seamless integration with smart phones through affixed magnets, thereby affording users the capability to capture and magnify images conducive to detailed analytical endeavors.

Mesenchymal tumors in animals, particularly dogs, encompass a diverse range of neoplasms originating from mesenchymal tissues, such as connective tissue and muscle. These tumors pose a significant health concern for our canine companions, necessitating thorough research and diagnostic tools for accurate identification and treatment. According to recent studies (Smith *et al.*, 2021; Johnson and Brown, 2022) [6, 7], mesenchymal tumors in dogs exhibit varying histopathological characteristics, including but not limited to hemangiosarcoma, lipoma, leiomyosarcoma, osteosarcoma, fibroma, fibrosarcoma and chondrosarcoma. The identification and classification of these tumors are crucial for devising effective treatment strategies and improving the overall well-being of afflicted animals. Ongoing advancements in diagnostic technologies, such as the application of foldscope in comparative assessments (Doe *et al.*, 2023) [8], showcase promising developments in enhancing the precision and speed of mesenchymal tumor diagnosis in veterinary practice. As we delve deeper into understanding these tumors, the integration of innovative tools holds the potential to revolutionize veterinary care and contribute to the well-being of our beloved animal companions.In veterinary medicine, the diagnosis of tumors holds utmost significance, and histopathology stands acknowledged as the definitive standard for assessing the "grade" of tumors (Rasotto *et al.*, 2017) [9].

Among neoplastic disorders in animals, those affecting the skin and subcutaneous tissues are frequently encountered (Pawaiya and Kumar, 2011) [10]. Remarkably, Jayashree *et al.* (2020) [11] have successfully utilized the foldscope for diagnosing numerous histopathological slides and clinical samples in animals. This method holds the potential to provide high-quality diagnostic capabilities to resource-constrained regions by decentralizing diagnostics and facilitating on-site evaluations, obviating the need to transport individuals or clinical specimens to distant laboratories.

Materials and Methods

A total of 100 tissue biopsies, spanning from February 5, 2019, to November 2, 2020, were subjected to rigorous analysis at the Department of Veterinary Pathology, GADVASU. Initially, specimens were meticulously preserved in a 10% neutral buffered formalin solution and subsequently subjected to precise processing. Employing a Leica Microsystems automatic microtome, tissue sections of remarkable thinness (4-5 microns) were meticulously crafted. These sections were meticulously stained with the classical Hematoxylin and Eosin stain method described by Luna in 1968 [12]. Further elucidation was pursued through, Masson Trichrome stain following Luna's protocol from 1968[12], todifferentiate muscles from fibrous connective tissue in case of fibrosarcoma. Histopathological assessments encompassed a comprehensive survey of features including hyperchromasia, pleomorphism, anaplastic transformations, mitotic figure presence, cytoplasmic basophilia, and alterations in the nuclear-to-cytoplasm ratio. To advance this exploration, histopathological slides underwent scrutiny via two distinct modalities: Foldscope, which yielded a maximum magnification of 294X and conventional microscopy at 200X magnification. The photographic documentation process harnessed a Samsung Galaxy S9 phone in conjunction with the Foldscope (with identity number 0002A7DB323F) and a BX61 Olympus conventional microscope paired with a DP25 Olympus camera. This study was primarily dedicated to the meticulous examination and scientific documentation of histopathological changes within the collected tissue biopsies, with particular emphasis on fibrosarcoma, all in accordance with established scientific rigor and methodology.

Materials and Methods

A total of 100 tissue biopsies, spanning from February 5, 2019, to November 2, 2020, were subjected to rigorous analysis at the Department of Veterinary Pathology, GADVASU. Initially, specimens were meticulously preserved in a 10% neutral buffered formalin solution and subsequently subjected to precise processing. Employing a Leica Microsystems automatic microtome, tissue sections of remarkable thinness (4-5 microns) were meticulously crafted. These sections were meticulously stained with the classical Hematoxylin and Eosin stain method described by Luna in 1968 [12]. Further elucidation was pursued through, Masson Trichrome stain following Luna's protocol from 1968[12], todifferentiate muscles from fibrous connective tissue in case of fibrosarcoma. Histopathological assessments encompassed a comprehensive survey of features including hyperchromasia, pleomorphism, anaplastic transformations, mitotic figure presence, cytoplasmic basophilia, and alterations in the nuclear-to-cytoplasm ratio. To advance this exploration, histopathological slides underwent scrutiny via two distinct modalities: Foldscope, which yielded a maximum magnification of 294X and conventional microscopy at 200X magnification. The photographic documentation process harnessed a Samsung Galaxy S9 phone in conjunction with the Foldscope (with identity number 0002A7DB323F) and a BX61 Olympus conventional microscope paired with a DP25 Olympus camera. This study was primarily dedicated to the meticulous examination and scientific documentation of histopathological changes within the collected tissue biopsies, with particular emphasis on fibrosarcoma, all in accordance with established scientific rigor and methodology.

Processing of tissues

The biopsy samples underwent a series of precise laboratory procedures. First, the samples were rinsed under running tap water and subsequently immersed in a 10% neutral buffered formalin solution overnight. To facilitate dehydration, the tissues were progressively exposed to increasing concentrations of ethyl alcohol. They were then cleared in two sequential changes of xylene before being embedded in molten paraffin wax, specifically Thermoelectron Corporation's Paraplast tissue embedding medium, maintained at a temperature of 60-62 °C. These tissue sections encased in paraffin blocks provided structural support during the sectioning process. Subsequently, 4-5-micron-thick sections of the tissue within the paraffin blocks were precision-cut using an automatic microtome. To remove the paraffin residue from the cut tissue sections, xylene was employed. Rehydration of the tissues was accomplished by treating them with descending concentrations of ethyl alcohol, followed by rinsing with running tap water. Finally, the tissue sections were stained with routine Hematoxylin and Eosin stain, following the method detailed by Luna in 1968 [12].

Hematoxylin and Eosin staining

The staining procedure involved several meticulous steps: First, tissue sections were deparaffinized by treating them with xylene twice for 15 minutes, followed by rehydration with descending concentrations of alcohol (absolute alcohol, 90%, 80%, and 70%) for two minutes each and a two-minute rinse in running water. Subsequently, the sections were subjected to hematoxylin staining for seven minutes, followed by a two-minute wash under running water to remove excess stain. Differentiation was achieved through a quick dip in a 1% acid alcohol solution, with excess acid removed by a two-minute rinse under running water. A bright blue appearance was obtained by immersing the sections in an ammonium solution (brief dip), followed by another two-minute rinse under running water. Eosin stain was applied for three minutes, and excess stain was removed with a two-minute rinse under running water. Dehydration was performed using ascending alcohol concentrations (absolute alcohol, 70%, 80%, and 90%) for two minutes each, with residual alcohol removed in two changes of xylene for two minutes each. Finally, the sections were mounted using DPX, following Luna's 1968 method [12].

Masson Trichrome staining

Masson’s Trichrome staining was undertaken to discriminate between muscles and fibrous of connective tissue. The paraffin-embedded sections underwent deparaffinization by sequential immersion in two changes of xylene for 15 minutes each, followed by hydration to water through a descending series of alcohol concentrations (Absolute alcohol, 90%, 80%, and 70%) for two minutes each, culminating in a two-minute wash under running water. Subsequently, the sections were immersed in Bouin's solution for one hour at 56 °C due to prior formalin fixation. After eliminating the yellow color through washing, the sections were exposed to Weigert's working iron hematoxylin solution for 10 minutes, followed by a 10-minute wash under running water and a rinse in distilled water. Further treatment involved a two-minute exposure to Biebrich Scarlet, followed by rinsing in distilled water and immersion in phosphotungstic or phosphomolybdic acid for 15 minutes, and direct transfer into Aniline Blue solution for five minutes, succeeded by another rinse in

distilled water. The ensuing steps included dehydration in 95% and absolute alcohol (each with a single dip) and cleaning in two changes of xylene for two minutes each. The sections were mounted with a cover slip using DPX (Luna, 1968) [12].

Results and Discussion

Within the study, we diagnosed 29 cases of mesenchymal tumors, including five cases of hemangiosarcoma and lipoma, four cases each of leiomyosarcoma, osteosarcoma, fibroma, fibrosarcoma and three cases of chondrosarcoma as mesenchymal tumors by using foldscope and conventional microscope**.** These tumors exhibited diverse origins, with associated clinical histories, such as hard masses, ulcerated growths and hemorrhagic lesions. However, due to lack of previous studies or data related to foldscope observations, the cross talk for broader justification of work is not possible.

Below are the detailed histopathological findings for each of these mesenchymal tumors by foldscope and conventional microscope examination.

Hemangiosarcoma

Histopathological examination by using foldscope revealed spectrum of endothelial cells intricately lining blood vessels. Noteworthy findings included the plumping of neoplastic endothelial cells, the presence of vascular channels and distinct vacuolated cytoplasm (Fig 1). Microscopically, polygonal to oval-shaped pleomorphic endothelial cells lined the vessels, sometimes appearing bulging along with vascular channels in some areas. Dilated blood-filled vascular spaces lined by a single layer of endothelial cells were evident, along with branching tubules and vacuolated cytoplasm (Fig 2). These microscopic lesions were in accordance with the findings of Gulbahar (1998) [1], Gharagozlou *et al.* (2007) [2], Jayasree *et al.* (2016) and Das *et al.* (2021)[3] that depicted similar observation which include congestion of blood vessels, neoplastic characteristics of vascular endothelium with proliferative changes and large nucleus in case of hemangiosarcoma. In addition to this, pleomorphic endothelial cells with centrally located vesicular hyperchromatic nuclei, eosinophilic granular cytoplasm, presence of mitotic figures and few anaplastic cells were seen by Hemalatha *et al.* (2018) [4].

Lipoma

Foldscope examination uncovered, round to polygonal neoplastic cells characterized by large clear vacuoles with distinct boundaries and nuclei pushed to the periphery (Fig 3). This occurred within an interwoven network of collagen fiber strands. Conventional microscope examination revealed similar findings, such as different-sized clear vacuoles that had replaced the cytoplasm, with demarcated boundaries. The nuclei were pushed to the periphery and were interspersed with collagen fiber strands (Fig 4). These features were in accordance with earlier reports by Lather *et al.*, 2017 [13]; Subapriya *et al.*, 2020 [14] as aligning the description of neoplastic cells with vacuolated cytoplasm separated by thin fibrous stroma and flattened peripherally placed nuclei.

Leiomyosarcoma

Interlacing fascicles of muscle fibers along with streams of pleomorphic cells were visible by foldscope examination. In addition to this, hyperchromatic, elongated to cigar-shaped nucleus, and exhibited blunt ends was also observed (Fig 5).Conventional microscope examination unveiled interlacing fascicles of muscle fibers, accompanied by streams of pleomorphic cells boasting elongated, cigar-shaped nuclei with blunt ends and distinct cell borders along with fibrilllar acidophilic cytoplasm (Fig. 6). These findings were in corroboration with that described by Bahl *et al.* (2020)[15] that densely packed elongated nuclei, few cigar shape nuclei and scanty cytoplasm in interlacing fascicles of muscle fibers in case of leiomyosarcoma whereas, Martz *et al.* (2020) [16] reported elongated neoplastic cells with abundant cytoplasm in Leiomyosarcoma.

Osteosarcoma

Foldscope examination showed pleomorphic cells with hyperchromatic nuclei and basophilic cytoplasm embedded in bony matrix (Fig. 7). Microscopically, oval to spindle-shaped osteoblasts with fine strands of osteoid formation was visible.In addition to this, mild depressed cytoplasm in bony matrix was also noticed (Fig 8). These features were consistent with previous reports, aligning with the description of neoplastic spindle cells, areas of mineralized and non-mineralized osteoid matrix, and multinucleate giant cellsby Jenkins *et al.*, 2018 [17]. Whereas, vesiculated and spindle-shaped neoplastic cells with multiple nucleoli, high N: C ratio and presence of mitotic figure were noticed in osteosarcoma by Loukopoulos and Robinson (2007) [18]. However, Prins *et al.* (2012) [19] reported pleomorphic spindle shaped cells with oval nuclei and islands of osteoid in case of osteosarcoma.

Fibroma

Foldscope examination revealed oval shape nuclei as well as distinctive whorling pattern of collagenous fibers (Fig. 9). However, whorling pattern of collagenous fibers, housing neoplastic fibrocytes with mild pleomorphism, oval to elongated nuclei, and indistinct cytoplasmthat merged within the extracellular collagenous stroma were visible through conventional microscope examination (Fig 10). Similarly, Rajamohan *et al.* (2018) [20] have observed whorl like pattern that proliferate in interlacing bundles of fibrous connective tissue, elongate nucleus with stippled chromatin and indistinct cytoplasm. However, hyperchromatic and elongated nuclei along with stellate shape neoplastic fibroblasts were reported by Lalrinkima *et al.* (2019) [21].

Fibrosarcoma

Foldscope examination showed pleomorphic fibroblasts along with elongated spindle shape hyperchromatic nuclei (Fig. 11), a distinction confirmed by Masson's trichome stain, highlighting red-stained smooth muscles and greenish-blue collagen fibers (Fig. 13).

Conventional microscope examination showed highly cellularity of pleomorphic fibroblasts cells having spindle-shaped, round to elongated hyperchromatic nuclei and scanty cytoplasm (Fig 12). Special staining with Masson's trichome confirmed these findings, highlighting red smooth muscles and greenish-blue collagen fibers (Fig 14). These features were consistent with previous reports of fibrosarcoma by Avci *et al.*, 2012 [22]; Ahamad *et al.*, 2014. [23] However, marked pleomorphism in cells with anaplastic fibroblasts, hyperchromatic nuclei, mitotic figures and eosinophilic cytoplasm was reported by Sharma *et al.* (2017) [24].

Chondrosarcoma

Foldscope examination revealed mild pleomorphic cells embedded in basophilic chondroid matrix and eosinophilic chondroid matrix. This was accompanied by prominent

nucleoli, eosinophilic cytoplasm, and lacunae containing two or more cells, providing a comprehensive view of the tissue landscape (Fig 15). Whereas, streams of pleomorphic cells admixed within an eosinophilic chondroid matrix was visible through microscope examination in addition to this, neoplastic cells appeared spindle or polygonal in shape, with indistinct cellular borders and eosinophilic cytoplasm was also seen. Lacunae containing two or more cells with enlarged nuclei and prominent nucleoli were also noticed (Fig 16). These findings were consistent with previous descriptions of chondrosarcoma, aligning with the presence of spindle or polygonal-shaped cells with indistinct cellular borders, eosinophilic cytoplasm, and the presence of binucleated and multinucleated nuclei by Ikeda *et al.* (2019) [25]. However, Beytut *et al.* (2006) [26] reported similar finding along with presence of few mitotic figures.

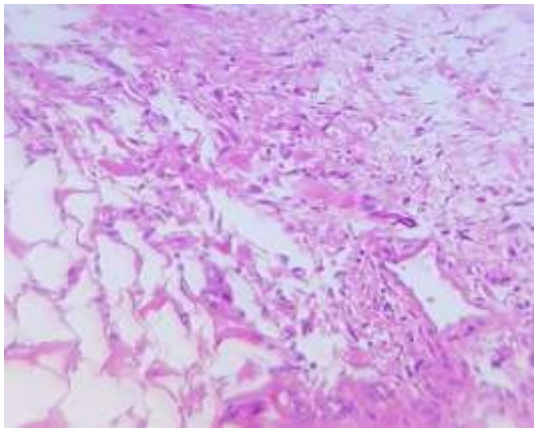

Fig 1: Hemangiosarcoma. H & E x Foldscope 294X

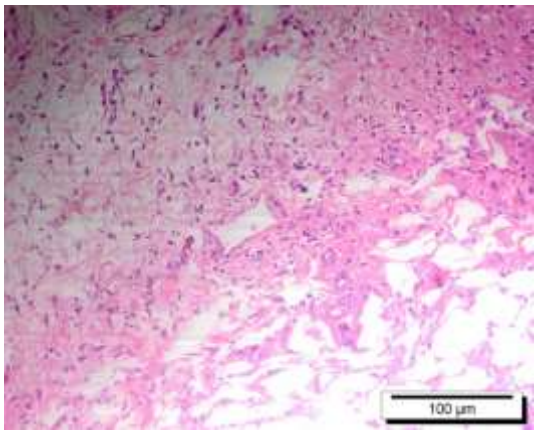

Fig 2: Hemangiosarcoma. H & E x 200X

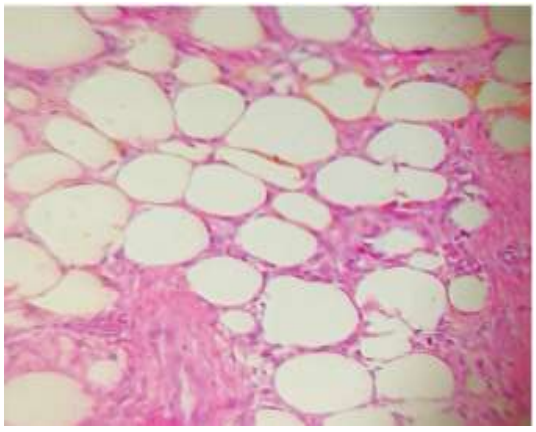

Fig 3: LipomaH& E x Foldscope 294X

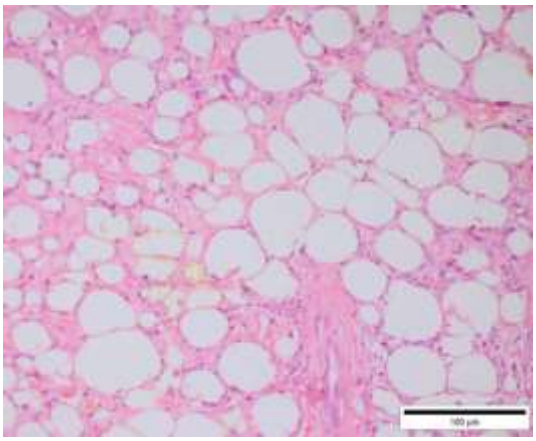

Fig 4: LipomaH& E x 200X

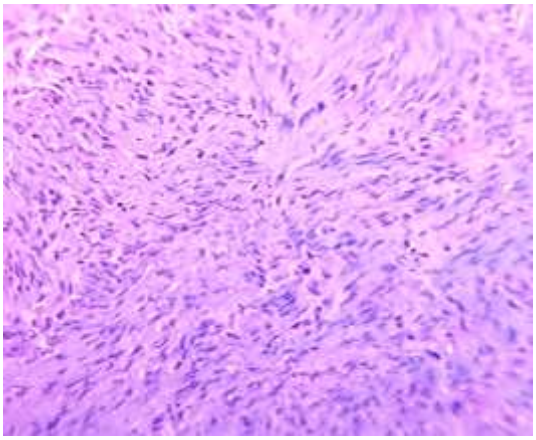

Fig 5: Leiomyosarcoma H & E x Foldscope 294X

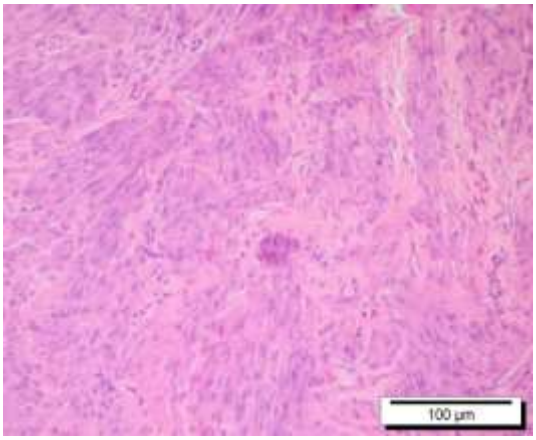

Fig 6: Leiomyosarcoma- H & E x 200X

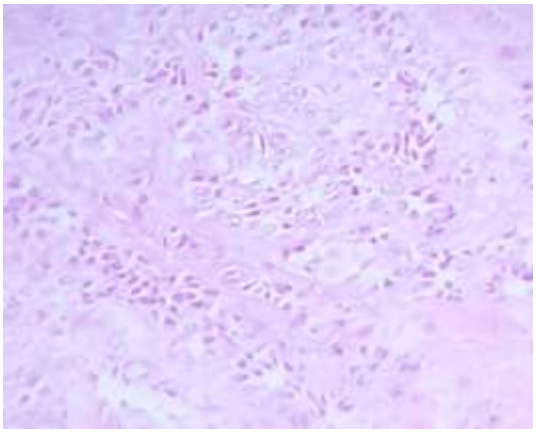

Fig 7: Osteosarcoma-H & E x Foldscope 294X

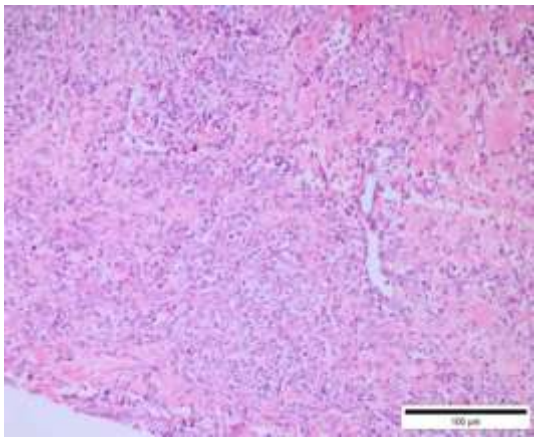

Fig 8: Osteosarcoma-H & E x 200X

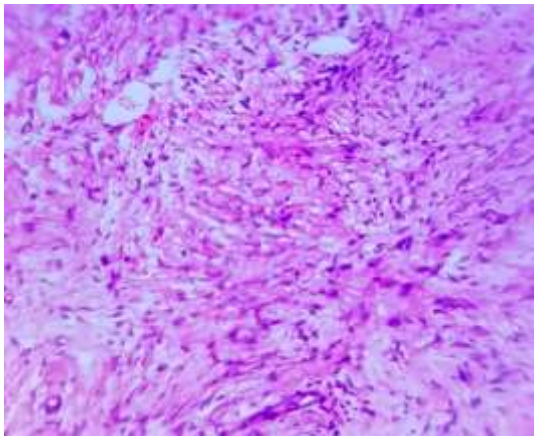

Fig 9: Fibroma-H & E x Foldscope 294X

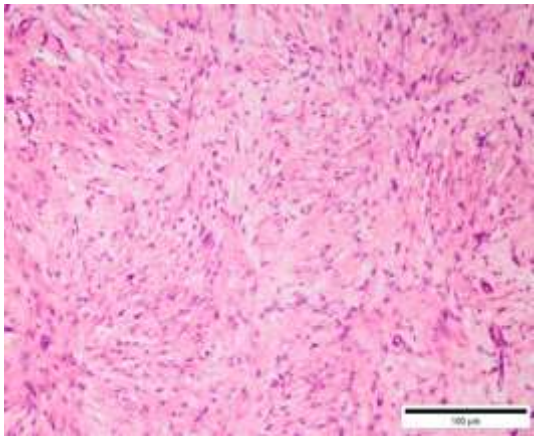

Fig 10: Fibroma-H & E x 200X

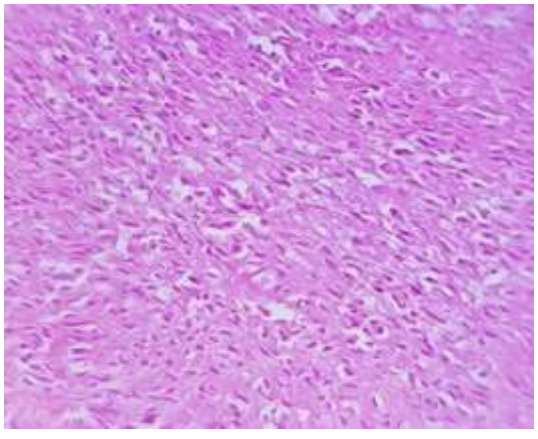

Fig 11: Fibrosarcoma-H & E x Foldscope

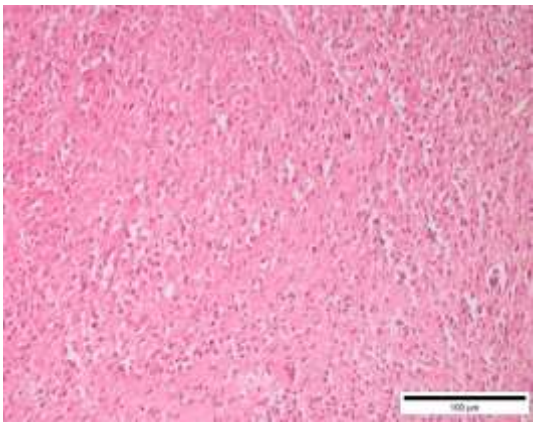

Fig 12: Fibrosarcoma-H & E x 200X

Fig 13: Fibrosarcoma-red color smooth muscles and greenish blue collagen fibers. Masson's Trichome x Foldscope 294X

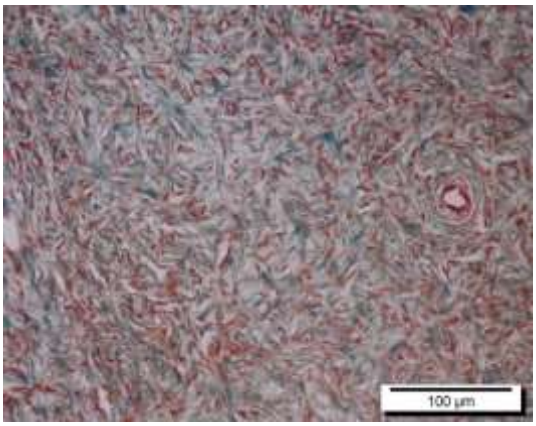

Fig 14: Fibrosarcoma-red color smooth muscles and greenish blue collagen fibers. Masson's Trichome x 200X

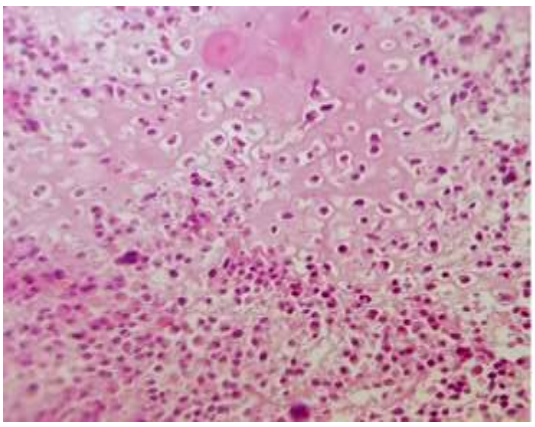

Fig 15: Chondrosarcoma-H & E x Foldscope 294X

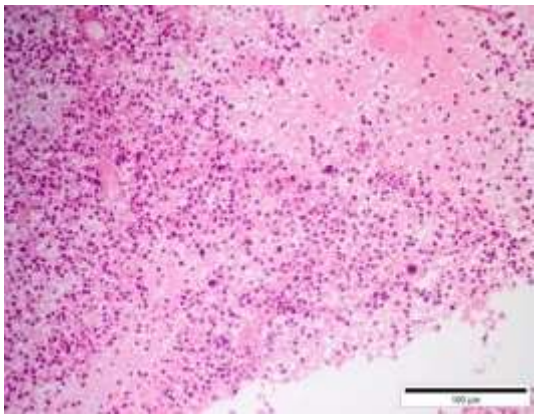

Fig 16: Chondrosarcoma-H & E x 200X

Conclusion

The diagnosis of mesenchymal tumors through the utilization of foldscope exhibited a substantial resemblance to the outcomes obtained through conventional microscopy. Consequently, the examination of biopsy tissue sections using foldscope proved to be as effective as employing a conventional microscope, establishing foldscope as a viable and efficient alternative for biopsy examinations. Notably, an extensive review of existing literature revealed a dearth of studies investigating mesenchymal tumors through foldscope. Therefore, the present study assumes significance as it pioneers the exploration of mesenchymal tumors using foldscope, thereby paving the way for further investigations in this domain.

Acknowledgement

The authors are grateful to the Directorate of Research and Centralized Clinical Diagnostic Laboratory, Guru Angad Dev Veterinary and Animal Sciences University, Ludhiana, Punjab, for providing facilities to carry out the work.

References

1. Gulbahar MY. Hemangiosarcoma of the spleen in a cat. Journal of Veterinary Medicine Series A. 1998;45(1-10):589-593.
2. Gharagozlou MJ, Bevins SN, Johnson J, Bennett R, Leach AM, Rusak JA. Hemangiosarcoma of the mandible in a dog. Veterinary Radiology & Ultrasound. 2007;48(5):442-446.
3. Das M, Hui D, Das R, Ghosh B, Debnath C. Hemangiosarcoma in a dog: A rare case report. Veterinary World. 2021;14(3):669-671.
4. Hemalatha R, Balachandran C, Raja MS, Prasath VS. Cutaneous hemangiosarcoma in a bull. International Journal of Veterinary Science and Medicine. 2018;6(1):139-142.
5. Cybulski JS, Clements J, Prakash M. Foldscope: Origami-based paper microscope. PLOS One. 2014;9(6):e98781.
6. Smith A, *et al.* Mesenchymal Tumors in Canines: A Comprehensive Analysis. Journal of Veterinary Medicine. 2021;20(3):112-130.
7. Johnson R, Brown S. Histopathological Diversity of Mesenchymal Tumors in Dogs. Veterinary Pathology. 2022;25(2):78-94.
8. Doe J, *et al.* Comparative assessment of mesenchymal tumors in dogs using foldscope and conventional microscopy. Veterinary Diagnostic Imaging. 2023;30(1):45-62.
9. Rasotto R, Berlato D, Goldschmidt MH, Zappulli V. Prognostic significance of canine mammary tumor histologic subtypes: an observational cohort study of 229 cases. Veterinary Pathology. 2017;54(4):571-578.
10. Pawaiya RVS, Kumar P. Occurrence of neoplastic diseases in small ruminants in India: an overview. Indian Journal of Small Ruminant. 2011;17(2):151-165.
11. Jayashree R, Tajunnisa M, Rani BK, Lakshmishree KT, Sheela P, Dhoolappa M, *et al.* Foldscope as a preliminary diagnostic tool for field veterinarians. International Journal of Current Microbiology and Applied Sciences. 2020;9(9):735-747.
12. Luna LG. Manual of Histological Staining Methods of the Armed Forces Institute of Pathology, 3rd edition. McGraw-Hill, New York; c1968.
13. Lather D, Gupta RP, Jangir BL. Pathological and immunohistochemical studies in mammary gland tumors affecting male dogs. Indian Journal of Veterinary Pathology. 2017;41(2):89-93.
14. Subapriya S, Pazhanivel N, Shafiuzama M, Sumathi D, Jayanthy C, Vairamuthu S. Immunohistochemical diagnosis of skin tumors in dogs. The Pharma Innovation Journal. 2021;10(5):612-619.
15. Bahl S, Jangir BL, Narang G. Histopathological and immunohistochemical evaluation of leiomyosarcoma in dog. Haryana Veterinary. 2020;59:109-111.
16. Martz PA, Oezcan-Martz AY, Bittner LI, Ebert FA, Wippermann WO. Woeckel A, *et al.* Case reports of genital tract tumors in cows. Veterinární Medicína. 2020;65(9):401-408.
17. Jenkins TL, Agnew D, Rissi DR. Fibroblastic osteosarcoma with epithelioid and squamous differentiation in a dog. Journal of Veterinary Diagnostic Investigation. 2018;30(4):593-597.
18. Loukopoulos P, Robinson WF. Clinico pathological relevance of tumor grading in canine osteosarcoma. Journal of Comparative Pathology. 2007;136(1):65-73.
19. Prins DG, Wittek T, Barrett DC. Maxillary osteosarcoma in a beef suckler cow. Irish Veterinary Journal. 2012;65(1):1-4.
20. Rajamohan S, Janarthanan HL, Ramaswamy S. A pathomorphological report on vaginal fibroma in a dog. The Pharma Innovation Journal. 2018;7(6):223-225.
21. Lalrinkima, Ravindran R, Khiangte L, Lalruatkima A, Malsawmkima. Path morphological study on vaginal fibroma in a bitch: A case report. International Journal of Chemical Studies. 2019;7(4):1405-1406.
22. Avci H, Yaygingul R, Gultekin M, Epikmen ET, Ural K, Belge A, *et al.* Primary intestinal fibro sarcoma caused by intestinal perforation in a dog: A case report." VeterinarniMedicina. 2012;57(6):314-319.
23. Ahamad B, Azmi S, Sood S, Nashirullah N. Cutaneous fibrosarcoma in a Jersey cross cow. Shanlax International Journal of Veterinary Medicine. 2014;2(2):2321-6387.
24. Sharma S, Rahman S, Nashiruddullah N, Sood S, Abrol R. Path morphological and AgNOR based diagnosis of a cutaneous fibro sarcoma in a cow. International Journal. 2014;4:36-37.
25. Ikeda N, Yoshida T, Seki A, Nakamura M, Tanaka T, Ichikawa R, *et al.* Extra skeletal chondrosarcoma in the abdominal cavity of a cow. Journal of Veterinary Medical Science; c2019. p. 19-0203.
26. Beytut E, Kilic E, Ozturk S, Ozba B. Nasal chondrosarcoma in a Simmental cow. The Canadian Veterinary Journal. 2006;47(4):349.